TECHNICAL PAPER
Journal of the South African Institution of Civil Engineering, 46(3) 2004, Pages 10–15, Paper 575

On analytical solutions for liquid-filled non-shallow conical shell assemblies

A Zingoni

Alphose Zingoni is professor of structural engineering and mechanics in the Department of Civil Engineering of the University of Cape Town. He holds an MSc degree in structural engineering and a PhD degree in shell structures, both awarded by Imperial College of Science, Technology and Medicine in the UK. His research interests encompass shell structures, space structures and applications of group theory to computational problems in structural mechanics. He has written a book on shell structures, published in the UK in 1997 by Thomas Telford (Institution of Civil Engineers), and has authored more than 60 papers in refereed international journals and conference proceedings. Professor Zingoni serves on several international committees and editorial boards and is a chartered structural engineer.

Keywords: conical shells, shells of revolution, shell structures, containment shells, shell analysis, shell design

On the basis of linear elastic shell theory, analytical results for stresses and deformations in liquid-filled conical shell assemblies are presented. For these structural configurations, which find application in elevated liquid containment and pressure vessels, such complete sets of closed-form results have never been presented before in the literature, to the author's best knowledge. The membrane solution is adopted as the particular solution of the bending-theory equations, while the one-term asymptotic-series solution for the axisymmetric bending of a non-shallow thin conical shell serves as the homogeneous component of the total solution, allowing all stresses and deformations to be conveniently obtained in closed form. These analytical results, used in combination with numerical analyses such as the finite-element method, permit a rapid and efficient analysis and design of the shell structures in question. The presented results have the added value of serving as a convenient benchmark for checking the performance of numerical formulations for problems of the type under discussion. A numerical example illustrates the value of the analytical results as a tool for parametric study and design.

INTRODUCTION

Conical shell assemblies are widely used as pressure vessels and liquid-containment vessels in the processing, manufacturing, transportation and construction industries. In view of their widespread application, it is useful for the structural designer to have, wherever possible, readily usable sets of analytical results for effects such as stresses and deformations. Such closed-form results, used in combination with numerical techniques such as the finite element method, permit a rapid and efficient analysis and design of the shell structures in question.

Numerous studies on conical shells have been undertaken by earlier investigators. Of particular significance were those studies concerned with axisymmetrically loaded thin conical frusta

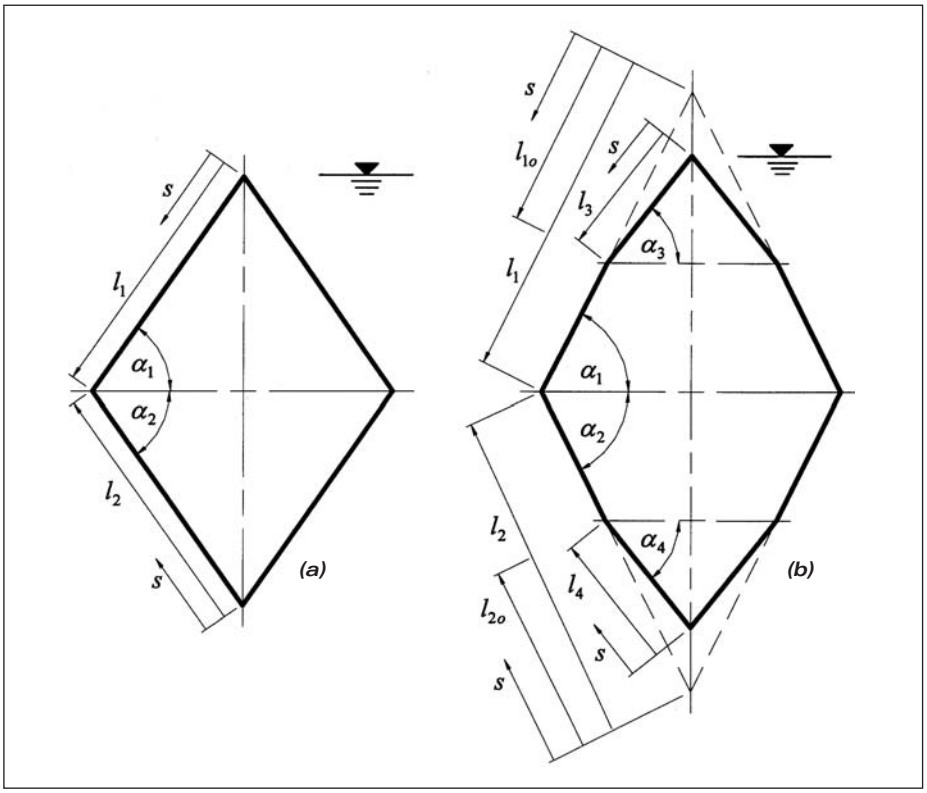

Figure 1 Two configurations of liquid-filled conical shell assemblies: (a) two-cone assembly; (b) four-cone assembly

(Baltrukonis 1959), where the focus was on quantifying the effects arising at the edges as well as in interior locations of such shells, when the edges were subjected to arbitrary sets of axisymmetric bending moments and shearing forces. Closed-form tabulations for stresses and deformations in isolated conical shells subjected to concentrated edge loads and distributed surface loads may be seen in the work of Baker *et al* (1972) and of Young (1989), among others. Hardly any such results exist in the literature on assemblies of conical shells, where the problem becomes more practical, and is dominated by junction effects. The underlying assumptions and theory of thin elastic shells are assumed to be familiar to the reader, and constitute established knowledge (Flugge 1973; Zingoni 1997).

In this contribution, with elevated closed-profile liquid-containment shell applications in mind, closed-form results for stresses and deformations are presented for two configurations of conical-shell assemblies depicted in figure 1. The configuration in figure 1(a) comprises two cones of meridional lengths $\{l_1, l_2\}$ and base angles $\{\alpha_1, \alpha_2\}$, connected at their open ends as shown in the figure, with s denoting the distance coordinate along the inclined shell meridian, measured from the respective vertex. These two cones will be referred to as Shell 1 (upper cone) and Shell 2 (lower cone). The configuration in figure 1(b) comprises two middle conical frusta whose extended sides form cones of meridional lengths $\{l_1, l_2\}$ with base angles $\{\alpha_1, \alpha_2\}$, connected together at their wider ends as shown in the figure. These frusta are joined at their narrower ends to conical shells of meridional lengths $\{l_3, l_4\}$ and base angles $\{\alpha_3, \alpha_4\}$. For this second configuration, we will refer to the upper and lower middle frusta as Shells 1 and 2 respectively, and the upper and lower conical end closures as Shells 3 and 4 respectively. The position of any point on the assembly will be defined by the distance coordinate s, which will be measured from the vertex of the cone on which the point lies, as shown in the diagrams. The thickness t of each shell, which may vary from point to point along the shell profile, is assumed to be small in relation to the length l of the respective shell ($l/t \geq 30$), while the angle α must not be too small ($\alpha \geq 30^o$), for the results that will be presented to be reasonably accurate (errors less than 5 %).

The vessels are assumed to be filled to capacity with liquid of weight γ per unit volume, and vertically supported at or around the lower vertex. Herein, details of the support need not be specified, since we are concerned with only the membrane effects induced in the shells by the hydrostatic internal pressure of the liquid, and edge effects that arise at the junctions of the various shells; from Saint Venant's principle, and the generally very localised nature of edge effects in shells of revolution of positive or zero Gaussian curvature (ie synclastic and developable shells), the influence of the support on structural response over most of the assembly will be minimal. As is usual in tackling problems of this nature (Zingoni 1997), and without any significant loss of accuracy, the membrane solution is assumed to be the particular solution of the general bending-theory equations of the shell, and simply superimposed with the edge effects (homogeneous solution) to yield the net effects in the shell.

MEMBRANE EFFECTS

Stress resultants

The membrane stress resultants (internal forces per unit length) in a thin conical shell subjected to axisymmetric surface-loading components p_r (applied force per unit area in the direction normal to the shell midsurface) and p_s (applied force per unit area in the direction tangential to the shell meridian) are given by (Flugge 1973; Zingoni 1997)

$$N_s^m = \frac{1}{s}\left[\int (p_r \cot\alpha - p_s)s\,ds + k\right] \tag{1a}$$

$$N_\theta^m = s(\cot\alpha)p_r \tag{1b}$$

where N_s^m is the stress resultant in the meridional direction (ie the direction along which s is measured) and N_θ^m the stress resultant in the hoop (ie circumferential) direction, these being considered positive when tensile; the superscript m will generally be used to denote membrane-solution quantities, to distinguish these from bending or edge effects. The parameter k is a constant of integration to be determined from an appropriate boundary condition; s and α are as already defined. For the loading under study, p_r is positive (since it acts outwards) and of magnitude equal to the hydrostatic pressure at a given point (ie $p_r = \gamma h$, where h is the depth of liquid at the point, and γ the weight density of the liquid as previously defined), while the component p_s is, of course, zero. The axisymmetry of both the shell geometry and the loading implies that membrane shear effects are absent.

For the uppermost shell of a configuration (ie Shell 1 in the configuration of figure 1(a) and Shell 3 in the configuration of figure 1(b)), k may be obtained from the usual condition of the finiteness of N_s at the vertex ($s = 0$). For the lower shells (ie Shell 2 in the configuration of figure 1(a) and Shells 1, 2 and 4 in the configuration of figure 1(b)), k is obtained here by enforcing vertical equilibrium at the upper edge of the shell in question (ie the vertical components of the N_s forces of the meeting shells must balance); horizontal equilibrium need not be satisfied, as any out-of-balance force will be accounted for by a ring beam and/or the bending-disturbance effects of the shell. Application of equations 1a and 1b, and these considerations for k, lead to the following results for the membrane stress resultants in the various shells (refer to figure 1 for the parameters occurring in these expressions):

Two-cone assembly

Shell 1 (upper cone): $0 \leq s \leq l_1$

$$N_s^m = \frac{\gamma}{3}(\cos\alpha_1)s^2 \tag{2a}$$

$$N_\theta^m = \gamma(\cos\alpha_1)s^2 \tag{2b}$$

Shell 2 (lower cone): $s \leq l_2$

$$N_s^m = \frac{1}{s}\left[\frac{\gamma}{2}(l_1\sin\alpha_1 + l_2\sin\alpha_2)(\cot\alpha_2)s^2 - \frac{\gamma}{3}(\cot\alpha_2)s^3 + k_2\right] \tag{3a}$$

$$N_\theta^m = \gamma(\cot\alpha_2)\left[(l_1\sin\alpha_1 + l_2\sin\alpha_2)s - (\sin\alpha_2)s^2\right] \tag{3b}$$

$$k_2 = \frac{\gamma}{3}l_2l_1^2\left(\frac{\sin\alpha_1\cos\alpha_1}{\sin\alpha_2}\right) - \frac{\gamma}{2}l_2^2(\cot\alpha_2)(l_1\sin\alpha_1 + l_2\sin\alpha_2) + \frac{\gamma}{3}l_2^3\cos\alpha_2 \tag{3c}$$

Four-cone assembly

The results are best presented for the shells from top to bottom (ie in the order Shell 3, Shell 1, Shell 2, Shell 4), since the k_i (i = 1, ..., 4) are evaluated in this order:

Shell 3 (uppermost cone): $0 \leq s \leq l_3$

$$N_s^m = \frac{\gamma}{3}(\cos\alpha_3)s^2 \tag{4a}$$

$$N_\theta^m = \gamma(\cos\alpha_3)s^2 \tag{4b}$$

Shell 1 (upper conical frustum): $l_{1o} \leq s \leq l_1$

$$N_s^m = \frac{1}{s}\left[(\gamma\cot\alpha_1)\left\{\frac{1}{3}(\sin\alpha_1)s^3 - \frac{1}{2}(l_{1o}\sin\alpha_1 - l_3\sin\alpha_3)s^2\right\} + k_1\right] \tag{5a}$$

$$N_\theta^m = \gamma(\cot\alpha_1)\left\{(\sin\alpha_1)s^2 - (l_{1o}\sin\alpha_1 - l_3\sin\alpha_3)s\right\} \tag{5b}$$

$$k_1 = \frac{\gamma}{3}l_{1o}l_3^2\left(\frac{\sin\alpha_3\cos\alpha_3}{\sin\alpha_1}\right) + \frac{\gamma}{2}l_{1o}^2(\cot\alpha_1)(l_{1o}\sin\alpha_1 - l_3\sin\alpha_3) - \frac{\gamma}{3}l_{1o}^3\cos\alpha_1 \tag{5c}$$

Shell 2 (lower conical frustum): $l_{2o} \leq s \leq l_2$

$$N_s^m = \frac{1}{s}\left[\frac{\gamma}{2}\{(l_1 - l_{1o})\sin\alpha_1 + l_2\sin\alpha_2 + l_3\sin\alpha_3\}(\cot\alpha_2)s^2 - \frac{\gamma}{3}(\cot\alpha_2)s^3 + k_2\right] \tag{6a}$$

$$N_\theta^m = \gamma(\cot\alpha_2)\left[\{(l_1 - l_{1o})\sin\alpha_1 + l_2\sin\alpha_2 + l_3\sin\alpha_3\}s - (\sin\alpha_2)s^2\right] \quad (6b)$$

$$k_2 = \gamma l_2\left(\frac{\cos\alpha_1}{\sin\alpha_2}\right)\left\{\frac{1}{3}l_1^2\sin\alpha_1 - \frac{1}{2}l_1(l_{1o}\sin\alpha_1 - l_3\sin\alpha_3)\right\} + \frac{l_2}{l_1}\left(\frac{\sin\alpha_1}{\sin\alpha_2}\right)k_1$$
$$-\frac{\gamma}{2}l_2^2(\cot\alpha_2)\{(l_1 - l_{1o})\sin\alpha_1 + l_2\sin\alpha_2 + l_3\sin\alpha_3\} + \frac{\gamma}{3}l_2^3\cos\alpha_2 \quad (6c)$$

Shell 4 (lowermost cone): $s \le l_4$

$$N_s^m = \frac{1}{s}\left[\frac{\gamma}{2}\{(l_1 - l_{1o})\sin\alpha_1 + (l_2 - l_{2o})\sin\alpha_2 + l_3\sin\alpha_3 + l_4\sin\alpha_4\}(\cot\alpha_4)s^2 - \frac{\gamma}{3}(\cot\alpha_4)s^3 + k_4\right] \quad (7a)$$

$$N_\theta^m = \gamma(\cot\alpha_4)\left[\{(l_1 - l_{1o})\sin\alpha_1 + (l_2 - l_{2o})\sin\alpha_2 + l_3\sin\alpha_3 + l_4\sin\alpha_4\}s - (\sin\alpha_4)s^2\right] \quad (7b)$$

$$k_4 = \gamma l_4\left(\frac{\cos\alpha_2}{\sin\alpha_4}\right)\left[\frac{1}{2}l_{2o}\{(l_1 - l_{1o})\sin\alpha_1 + l_2\sin\alpha_2 + l_3\sin\alpha_3\} - \frac{1}{3}l_{2o}^2\sin\alpha_2\right] + \frac{l_4}{l_{2o}}\left(\frac{\sin\alpha_2}{\sin\alpha_4}\right) - \frac{\gamma}{2}l_4^2(\cot\alpha_4)\{(l_1 - l_{1o})\sin\alpha_1 + (l_2 - l_{2o})\sin\alpha_2 + l_3\sin\alpha_3 + l_4\sin\alpha_4\} + \frac{\gamma}{3}l_4^3\cos\alpha_4 \quad (7c)$$

Edge values

In later calculations for edge effects at the central or 'equatorial' junction (ie the junction of Shells 1 and 2 for either of the two configurations in figure 1), the values of the membrane meridional stress resultant N_s^m at the edges of Shells 1 and 2 adjoining this junction will be required. For Shells 1 and 2, these will be denoted by N_{s1}^m and N_{s2}^m respectively. To obtain N_{s1}^m, we simply set s equal to l_1 in equation 2a for the two-cone configuration and in equation 5a for the four-cone configuration, with N_{s2}^m then immediately following from the earlier indicated condition of vertical equilibrium (namely that the vertical components of the N_s forces of the meeting shells must balance). The results are as follows:

Two-cone assembly

$$N_{s1}^m = \frac{\gamma}{3}(\cos\alpha_1)l_1^2 \quad (8a)$$

$$N_{s2}^m = \frac{\sin\alpha_1}{\sin\alpha_2}N_{s1}^m \quad (8b)$$

Four-cone assembly

$$N_{s1}^m = (\gamma\cot\alpha_1)\left\{\frac{1}{3}(\sin\alpha_1)l_1^2 - \frac{1}{2}(l_{1o}\sin\alpha_1 - l_3\sin\alpha_3)l_1\right\} + \frac{k_1}{l_1} \quad (9a)$$

$$N_{s2}^m = \frac{\sin\alpha_1}{\sin\alpha_2}N_{s1}^m \quad (9b)$$

Deformations

Denoting with δ the (horizontal) displacement perpendicular to the vertical axis of revolution of the shell (δ being positive when away from the axis of revolution), and with V the rotation of the shell meridian in the meridional section (positive when *anticlockwise* as viewed to the left of the vertical axis of symmetry, when the vertex of the cone lies *above* the opening of the cone, and positive when *clockwise* as viewed to the left of the vertical axis of symmetry, when the vertex lies *below* the opening of the cone), we may write membrane deformations in terms of membrane stress resultants as follows (Zingoni 1997):

$$\delta^m = \frac{1}{Et}(s\cos\alpha)\left(N_\theta^m - \nu N_s^m\right) \quad (10a)$$

$$V^m = (\cot\alpha)\left[\frac{1}{Et}(1+\nu)\left(N_s^m - N_\theta^m\right) - s\frac{d}{ds}\left\{\frac{1}{Et}\left(N_\theta^m - \nu N_s^m\right)\right\}\right] \quad (10b)$$

where t is the shell thickness at the point in question, E the Young modulus and ν the Poisson ratio of the shell material. Of particular interest are the deformations at the central or 'equatorial' junction, where Shells 1 and 2 (in either of the two configurations of figure 1) meet, which are required in the computation of the bending disturbances associated with this junction. They may be obtained on the basis of equations 10a and 10b, using the appropriate expressions for N_s^m and N_θ^m for the shell in question, and setting s equal to l_1 for Shell 1 and l_2 for Shell 2 in the final expressions. In applying equation 10b, the thickness t of the shell will be assumed to be constant. (Even if the thickness of the shell actually varies, this simplification will not affect the final stresses significantly, as long as the variation is not too rapid.) The results are as follows, with subscripts 1 and 2 denoting parameters of Shells 1 and 2 respectively:

Two-cone assembly

$$\delta_1^m = \frac{1}{3}\frac{\gamma l_1^3}{Et_1}(3-\nu)(\cos^2\alpha_1) \quad (11a)$$

$$V_1^m = -\frac{8}{3}\frac{\gamma l_1^2}{Et_1}\frac{\cos^2\alpha_1}{\sin\alpha_1} \quad (11b)$$

$$\delta_2^m = \frac{1}{Et_2}(l_2\cos\alpha_2)\left[\gamma(\cot\alpha_2)\{(l_1\sin\alpha_1 + l_2\sin\alpha_2)l_2 - (\sin\alpha_2)l_2^2\} - \nu\left\{\frac{\gamma}{2}(\cot\alpha_2)(l_1\sin\alpha_1 + l_2\sin\alpha_2)l_2 - \frac{\gamma}{3}(\cos\alpha_2)l_2^2 + \frac{k_2}{l_2}\right\}\right] \quad (12a)$$

$$V_2^m = \frac{1}{Et_2}(\cot\alpha_2)\left\{-\frac{3}{2}\gamma l_1 l_2(\sin\alpha_1\cot\alpha_2) + \frac{7}{6}\gamma l_2^2(\cos\alpha_2) + \frac{k_2}{l_2}\right\} \quad (12b)$$

Four-cone assembly

$$\delta_1^m = \frac{\gamma}{Et_1}l_1\left(\frac{\cos^2\alpha_1}{\sin\alpha_1}\right)\left[\{l_1^2(\sin\alpha_1) - l_1(l_{1o}\sin\alpha_1 - l_3\sin\alpha_3)\} - \nu\left\{\frac{1}{3}l_1^2(\sin\alpha_1) - \frac{1}{2}l_1(l_{1o}\sin\alpha_1 - l_3\sin\alpha_3) + \frac{k_1}{\gamma l_1\cot\alpha_1}\right\}\right] \quad (13a)$$

$$V_1^m = -\frac{\gamma}{Et_1}(\cot^2\alpha_1)\left\{\frac{8}{3}l_1^2(\sin\alpha_1) - \frac{3}{2}l_1 l_{1o}(\sin\alpha_1) + \frac{3}{2}l_1 l_3\sin\alpha_3 - \frac{k_1}{\gamma l_1\cot\alpha_1}\right\} \quad (13b)$$

$$\delta_2^m = \frac{\gamma}{Et_2}l_2\left(\frac{\cos^2\alpha_2}{\sin\alpha_2}\right)\left[\{l_2 l_3(\sin\alpha_3) + l_2(l_1 - l_{1o})\sin\alpha_1\} - \nu\left\{\frac{1}{2}l_2 l_3(\sin\alpha_3) + \frac{1}{2}l_2(l_1 - l_{1o})\sin\alpha_1 + \frac{1}{6}l_2^2\sin\alpha_2 + \frac{k_2}{\gamma l_2\cot\alpha_2}\right\}\right] \quad (14a)$$

$$V_2^m = -\frac{\gamma}{Et_2}(\cot^2\alpha_2)\left\{\frac{3}{2}l_2[l_3\sin\alpha_3 + (l_1 - l_{1o})\sin\alpha_1] - \frac{7}{6}l_2^2(\sin\alpha_2) - \frac{k_2}{\gamma l_2\cot\alpha_2}\right\} \quad (14b)$$

JUNCTION EFFECTS AND TOTAL STRESSES

For the estimation of edge-zone effects associated with the application of axisymmetric bending moments and shearing forces at the edge of a conical shell, an approximate approach, based on replacing the Bessel/Kelvin functions of the exact solution (to the axisymmetric bending problem of the conical shell) with their one-term asymptotic expan-

sions, has been developed in earlier work (Zingoni 2002). In particular, closed-form solutions for shell-edge redundants $\{M_1, H_1, M_2, H_2\}$ at the junction of two cones (Shells 1 and 2), with vertices lying on opposite sides of the junction plane, were obtained in terms of meridional membrane stress resultants $\{N_{s1}^m, N_{s2}^m\}$ at the shell edges, membrane edge deformations $\{V_1^m, \delta_1^m, V_2^m, \delta_2^m,\}$ and the geometric parameters $\{l_1, \alpha_1, t_1, l_2, \alpha_2, t_2\}$ of the two shells, for any arbitrary surface loadings on the two shells. The relevant conditions necessary for the evaluation of these four shell-edge redundants $\{M_1, H_1, M_2, H_2\}$ comprise horizontal-force and moment equilibrium of an element of the shell at the junction of the two meeting cones, namely

$$H_1 + H_2 - (N_{s1}^m \cos\alpha_1 + N_{s2}^m \cos\alpha_2) = 0 \tag{15a}$$

$$M_1 - M_2 = 0 \tag{15b}$$

and compatibility of net deformations $\{\delta^T, V^T\}$ between the upper and lower shells at their junction, namely

$$\delta_1^T (= \delta_1^b + \delta_1^m) = \delta_2^T (= \delta_2^b + \delta_2^m) \tag{16a}$$

$$V_1^T (= V_1^b + V_1^m) = -V_2^T \ (= -V_2^b - V_2^m) \tag{16b}$$

In these equations, and for the present problems, all the membrane-solution quantities are known (as already given in the previous section), while bending-related edge deformations $\{\delta_e^b, V_e^b\}$ due to arbitrary shell-edge actions $\{M_e, H_e\}$ may be seen in the earlier work (Zingoni 2002). In this section, we will summarise the results obtained by reference to the specific problems of the liquid-filled configurations of figure 1.

For the two shells meeting at the 'equatorial' junction of the whole assembly (ie Shells 1 and 2 of either of the configurations depicted in figure 1), let us define geometric parameters ω and β as follows ($i = 1$ for Shell 1; $i = 2$ for Shell 2):

$$\omega = 2\left[12(1-\nu^2)\frac{s^2}{t_i^2}\tan^2\alpha_i\right]^{1/4} \tag{17a}$$

$$\omega_i = (\omega)_{s=l_i} = 2\left[12(1-\nu^2)\frac{l_i^2}{t_i^2}\tan^2\alpha_i\right]^{1/4} \tag{17b}$$

$$\beta = \frac{\omega}{\sqrt{2}} \tag{18a}$$

$$\beta_i = (\beta)_{s=l_i} = \frac{\omega_i}{\sqrt{2}} \tag{18b}$$

Note that t_i is the constant thickness of Shell i. For a given Shell i ($i = 1$ or 2), ω and β are functions of s defined in the range $0 \le s \le l_i$ for the configuration of figure 1(a) and in the range $l_{io} \le s \le l_i$ for the configuration of figure 1(b), in both cases ω_i and β_i being the values of these parameters at the junction (ie when $s = l_i$).

Let us also define the following parameters, which are functions of $\{\omega_1, \omega_1\}$ and/or the membrane shell-edge quantities $\{N_{s1}^m, N_{s2}^m\}$, $\{\delta_1^m, \delta_2^m\}$ and $\{V_1^m, V_2^m\}$ for the configuration in question (fig 1(a) or fig 1(b)) as defined earlier in Section 2:

$$F_a = t_1 l_2 (\cos^2\alpha_2)(2\sqrt{2}\omega_2 - 4\nu) + t_2 l_1 (\cos^2\alpha_1)(2\sqrt{2}\omega_1 - 4\nu) \tag{19a}$$

$$F_b = 4Et_1t_2(\delta_2^m - \delta_1^m) \tag{19b}$$

$$F_c = t_1 l_2 (\cos^2\alpha_2)(2\sqrt{2}\omega_2 - 4\nu)(N_{s1}^m \cos\alpha_1 + N_{s2}^m \cos\alpha_2) \tag{19c}$$

$$\xi = \sqrt{2}\, t_1^2 (l_2 \sin\alpha_2)(N_{s1}^m \cos\alpha_1 + N_{s2}^m \cos\alpha_2) + \frac{Et_1^2t_2^2}{\sqrt{6(1-\nu^2)}}(V_1^m + V_2^m) \tag{19d}$$

$$\eta = \omega_1 t_2^2 + \omega_2 t_1^2 \tag{19e}$$

Then solutions for the shell-edge bending-moment and horizontal-shear redundants $\{M_1, H_1\}$ for Shell 1 and $\{M_2, H_2\}$ for Shell 2 may be written in the form

$$M_1 = \frac{(\sin\alpha_1)(\sin\alpha_2)\{\xi F_a + \sqrt{2}(t_1^2 l_2 \sin\alpha_2 - t_2^2 l_1 \sin\alpha_1)(F_b - F_c)\}}{\eta F_a (\sin\alpha)(\sin\alpha_2) + \sqrt{2}(t_1^2 l_2 \sin\alpha_2 - t_2^2 l_1 \sin\alpha_1)(t_2\omega_1^2 \sin\alpha_2 \cos^2\alpha_1 - t_1\omega_2^2 \sin\alpha_1 \cos^2\alpha_2)}$$

$$H_1 = \frac{\xi(t_2\omega_1^2 \sin\alpha_2 \cos^2\alpha_1 - t_1\omega_2^2 \sin\alpha_1 \cos^2\alpha_2) - \eta(\sin\alpha_1)(\sin\alpha_2)(F_b - F_c)}{\eta F_a (\sin\alpha_1)(\sin\alpha_2) + \sqrt{2}(t_1^2 l_2 \sin\alpha_2 - t_2^2 l_1 \sin\alpha_1)(t_2\omega_1^2 \sin\alpha_2 \cos^2\alpha_1 - t_1\omega_2^2 \sin\alpha_1 \cos^2\alpha_2)}$$

(20a, b)

$$M_2 = M_1 \tag{21a}$$

$$H_2 = (N_{s1}^m \cos\alpha_1 + N_{s2}^m \cos\alpha_2) - H_1 \tag{21b}$$

Shell-interior stress resultants $\{N_s^b, N_\theta^b\}$ (the superscript b denoting that these stress resultants are associated with the bending edge effects) and bending moments $\{M_s, M_\theta\}$ in the meridional and hoop directions, respectively, follow as (with, as before, $i = 1$ denoting Shell 1 variables and $i = 2$ denoting Shell 2 variables, the variables $\{s, \omega, \beta\}$ being, of course, those of the shell in question):

$$N_s^b = -\left(\frac{\cot\alpha_i}{s\sqrt{2}}\right)\left(\frac{\omega_i}{\omega}\right)^{1/2} e^{-(\beta_i - \beta)}$$
$$\left[\omega_i\{\sin(\beta_i - \beta)\}M_i + \sqrt{2}(l_i \sin\alpha_i)\{\cos(\beta_i - \beta) - \sin(\beta_i - \beta)\}H_i\right] \tag{22a}$$

$$N_\theta^b = -\left(\frac{\cot\alpha_i}{s2\sqrt{2}}\right)(\omega\omega_i)^{1/2} e^{-(\beta_i - \beta)}$$
$$\left[\frac{\omega_i}{\sqrt{2}}\{\sin(\beta_i - \beta) - \cos(\beta_i - \beta)\}M_i + (2l_i \sin\alpha_i)\{\cos(\beta_i - \beta)\}H_i\right] \tag{22b}$$

$$M_s = \frac{\sqrt{2}}{\omega}\left(\frac{\omega_i}{\omega}\right)^{1/2} e^{-(\beta_i - \beta)}$$
$$\left[\frac{\omega_i}{\sqrt{2}}\{\cos(\beta_i - \beta) + \sin(\beta_i - \beta)\}M_i - (2l_i \sin\alpha_i)\{\sin(\beta_i - \beta)\}H_i\right] \tag{22c}$$

$$M_\theta = \nu M_s \tag{22d}$$

Finally, the total stresses throughout Shells 1 and 2 are obtained by superimposing the stresses associated with the membrane solution with those associated with the bending edge effects, that is, for Shell i (where $i = 1$ for Shell 1 and $i = 2$ for Shell 2),

$$\sigma_s^T = \frac{N_s^b}{t} \pm \frac{6M_s}{t^2} + \frac{N_s^m}{t} \tag{23a}$$

$$\sigma_\theta^T = \frac{N_\theta^b}{t} \pm \frac{6M_\theta}{t^2} + \frac{N_\theta^m}{t} \tag{23b}$$

where σ_s^T refers to the meridional stresses, σ_θ^T refers to the hoop stresses, and t is, of course, the shell thickness; the upper and lower signs of ± refer to the inner and outer shell surfaces, respectively.

The reliability of the above analytical formulation has already been verified through comparisons with results of a finite-element analysis, where good agreement has been demonstrated (Zingoni 2002).

NUMERICAL EXAMPLE

Let us consider a rhombic two-cone assembly of overall height 40 m and equatorial diameter 20 m. The term 'rhombic' implies that the assembly is symmetric about the horizontal plane of intersection of the two cones, giving $\alpha_1 = \alpha_2 = 63{,}435^\circ$ and $l_1 = l_2 = 22{,}361$ m (refer to fig 1(a)). The thickness of the shell is assumed to be constant at 200 mm throughout (ie $t_1 = t_2 = 0{,}2$ m). The material of the shell has properties $E = 28 \times 10^9$ N/mm^2 and $\nu = 0{,}15$ (typical of concrete). The contained liquid is of weight per unit volume $\gamma = 9\,810$ N/m^3. The ves-

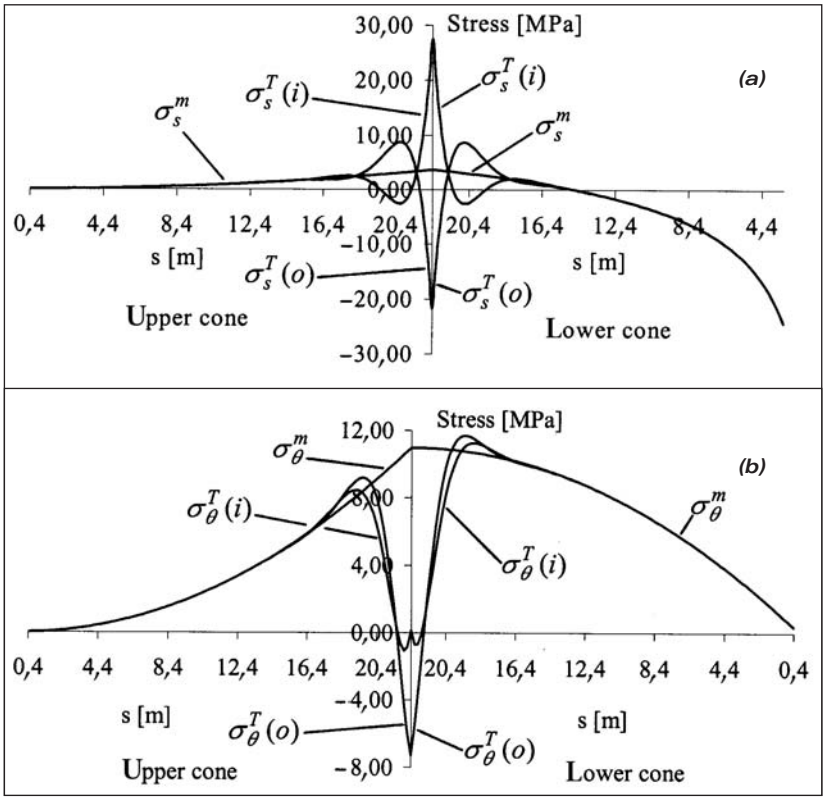

Figure 2 Variation of stresses around the equatorial junction for the two-cone rhombic configuration (numerical example): (a) meridional stresses; (b) hoop stresses

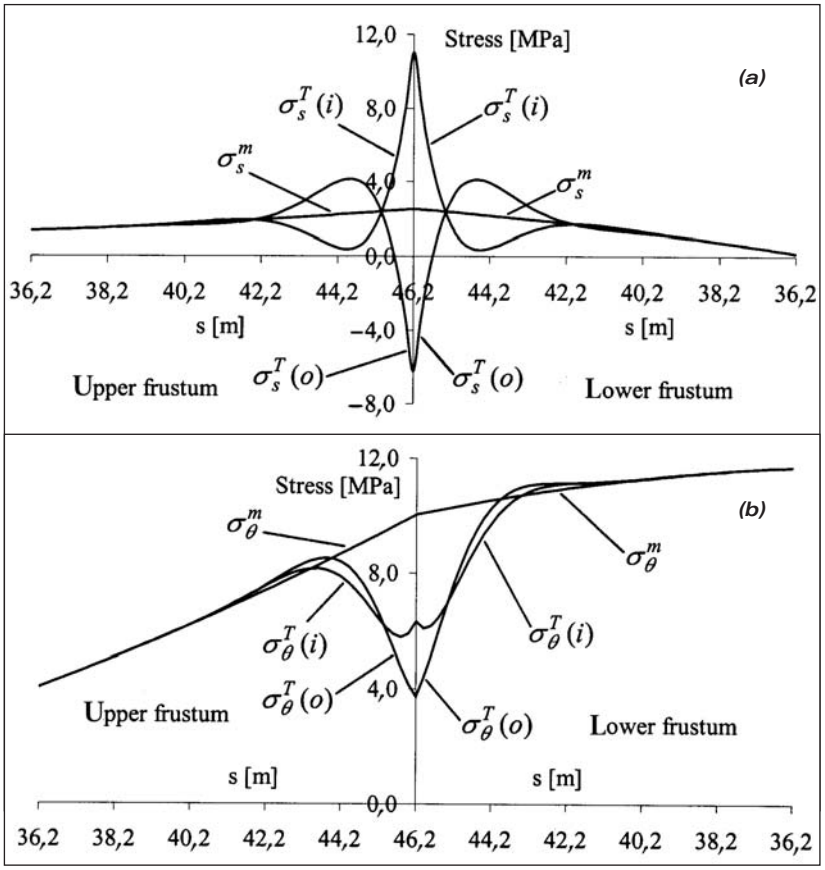

Figure 3 Variation of stresses around the equatorial junction for the four-cone configuration (numerical example): (a) meridional stresses; (b) hoop stresses

sel capacity works out at 4 189 m^3, which is not much for a containment structure of such a large height and diameter.

Let this arrangement be modified to a four-shell assembly (fig 1b) while preserving the overall height of 40 m and equatorial diameter of 20 m, and while aiming to keep the total angle subtended at the equatorial junction and at the upper and lower off-equatorial junctions about the same (ie the change in angle at the three junctions is the same in moving down the meridian from top to bottom), in order to 'balance out' discontinuity effects. This implies that $\alpha_1 = \alpha_2 = 77{,}5^o$ (giving a suitably obtuse subtended angle of 155^o at the equatorial junction, from the point of view of minimising junction effects there) and $\alpha_3 = \alpha_4 = 52{,}106^o$ (which is still sufficiently steep, from the point of view of prestressing the concrete shell). The length parameters work out at $l_1 = l_2 = 46{,}202$ m, $l_{1o} = l_{2o} = 35{,}960$ m and $l_3 = l_4 = 12{,}672$ m. As a result of this modification of the basic rhombic configuration, vessel capacity is enhanced considerably to 6 262 m^3.

Let us focus attention on the state of stress around the equatorial junction of each of the above two cases, since this is the location around which a high degree of bending would be expected to occur. Membrane stresses (σ^m), inner-surface total stresses ($\sigma^T(i)$) and outer-surface total stresses ($\sigma^T(o)$) are shown in figure 2 for the numerical example of the rhombic two-shell assembly and in figure 3 for the numerical example of the four-shell assembly. The stresses are plotted versus s, the distance coordinate from the vertex of the respective cone.

DISCUSSION OF NUMERICAL RESULTS

In shifting from the configuration of the rhombic two-shell assembly to the cone-frustum four-shell assembly, the membrane stresses at the equatorial junction reduce rather modestly from 3,5 MPa to 2,5 MPa (meridional stresses) and from 11,0 MPa to 10,0 MPa (hoop stresses). In terms of stress resultants N (= σt), these reductions are from 0,7 to 0,5 MN/m (meridional) and from 2,2 to 2,0 MN/m (hoop). Thus, comparing the rhombic configuration versus its cone-frustum variant, it is observed that not only is there a considerable gain in containment capacity (from 4 189 m^3 to 6 262 m^3) in adopting the latter over the former, but there is also the additional beneficial reduction in junction values of the membrane hoop stress resultant (from 2,2 to 2,0 MN/m), though this hoop stress resultant continues to rise gently to about 2,3 MN/m in moving from the equatorial junction towards the lower edge of the lower conical frustum. (In the simple rhombic configuration, the hoop tension decreases in moving down from the equatorial junction through the lower cone.)

Of greater significance is the effect on the discontinuity stresses of altering the conical configuration from simple rhombic to compound cone-frustal. Net meridional stresses at the junction reduce from 27,5 MPa to 11,0 MPa in tension, and from 22,0 MPa to 6,25 MPa in compression, which in terms of 'equivalent' stress resultants N (obtained by simply multiplying the total stress by the assumed shell thickness of t = 0,2 m, but as the total stress is actually a mixture of direct and flexural stresses, these equivalent stress resultants are not the real stress resultants in the shell), are reductions of 5,5 MN/m to 2,2 MN/m in tension, and 4,4 MN/m to 1,25 MN/m in compression. As is evident by reference to figures 2b and 3b, the bending disturbance at the equatorial junction has the effect of inducing hoop compression in the immediate vicinity of the junction, which in the case of the rhombic configuration results in a reversal of the hoop stresses at the junction from tensile (membrane) to compressive (net), but in the case of the compound cone-frustum assembly, the net hoop stresses at the junction still remain tensile but considerably reduced in magnitude.

SUMMARY AND CONCLUSIONS

Closed-form results for stresses and deformations in two practical configurations of conical shell assemblies have been presented. Effects distant from the junction locations have been calculated on the basis of the membrane solution only, while those at and in the vicinity of shell junctions are the result of superimposing the surface loading effects (associated with the membrane solution) with the edge effects (associated with the homogeneous bending solution). Although the solution approach adopted for the bending problem is only approximate, it is nevertheless sufficiently accurate for most applications encountered in the civil and mechanical engineering industries, provided that $\alpha \geq 30^{o}$ (where α is the base angle of the cone) and $l/t \geq 30$ (where l/t is the ratio of the sloping length of the cone to the shell thickness). As far as the author is aware, this is the first time a comprehensive set of practical analytical closed-form results for conical shell assemblies of the type in question has been presented, and these results are specifically applicable to problems of elevated liquid storage.

The results have been applied to the numerical example of a large conical assembly of overall-height to equatorial-diameter ratio of 2:1. From this numerical study, it has been observed that discontinuity effects at the junctions of the assemblies can be large in comparison with membrane stresses, and therefore should not be ignored. Modifying the simple rhombic two-shell configuration to a four-shell compound cone-frustum assembly (while preserving the overall height and diameter of the structure) not only enhances containment capacity, but also reduces the magnitude of the discontinuity stresses at the junctions quite significantly.

References

Baker, E H, Kovalevsky, L and Rish, F L 1972. *Structural analysis of shells*. New York: McGraw-Hill.

Baltrukonis, J H 1959. Influence coefficients for edge-loaded short thin conical frustums. ASME *Journal of Applied Mechanics*, 26(2).

Flugge, W 1973. *Stresses in shells*. Berlin: Springer-Verlag.

Young, W C 1989. *Roark's formulas for stress and strain*. New York: McGraw-Hill.

Zingoni, A 1997. *Shell structures in civil and mechanical engineering*. London: Thomas Telford.

Zingoni, A 2002. Discontinuity effects at cone-cone axisymmetric shell junctions. *Thin-Walled Structures*, 40(10): 877–891.